

Effects of Large-scale Moisture Transport and Mesoscale Processes on Precipitation Isotope Ratios Observed at Sumatera, Indonesia

Hironori FUDEYASU

Yokohama National University, Yokohama, Japan

Kimpei ICHIYANAGI

Kumamoto University, Kumamoto, Japan

Kei YOSHIMURA

University of Tokyo, Kashiwa, Japan

Shuichi MORI, HAMADA Jun-Ichi

Japan Agency for Marine-Earth Science and Technology (JAMSTEC), Yokosuka, Japan

Namiko SAKURAI

National Research Institute for Earth Science and Disaster Prevention (NIED), Tsukuba, Japan

Manabu D. YAMANAKA

*Japan Agency for Marine-Earth Science and Technology (JAMSTEC), Yokosuka, Japan
Kobe University, Kobe, Japan*

Jun MATSUMOTO

*Japan Agency for Marine-Earth Science and Technology (JAMSTEC), Yokosuka, Japan
Tokyo Metropolitan University, Hachioji, Japan*

and

Fadli SYAMSUDIN

Agency for the Assessment and Application of Technology (BPPT), Jakarta, Indonesia

(Manuscript received 30 April 2010, in final form 9 September 2010)

Abstract

Isotopic and meteorological observations in November 2006 on the west coast of Sumatera, Indonesia during the intense observation period of the Hydrometeorological ARray for Intraseasonal Variation-Monsoon AUtomonitoring (HARIMAU2006), revealed the impacts of large-scale moisture transport and mesoscale processes on precipitation isotope ratios. Intraseasonal changes in the precipitation $\delta^2\text{H}$ in November had large variability ranging from +10 to -65 per mil, as a result of the changes in the large-scale moisture transport associated with the intraseasonal oscillation with a time-scale of 10–15 day over Sumatera. The isotopic composition of precipitation was independent from difference in precipitation type (convective or stratiform precipitation). An isotope circulation model reproduced the observed isotopic changes, supporting that the isotopic effect of large-scale moisture transport was the main contributor to intraseasonal isotopic changes.

In high-frequency samples taken over a shorter time scale, isotopic variability was related to event type classified by the analysis of radar observations, although the isotopic effects of mesoscale processes on the isotopic averages of each precipitation event were almost masked by the isotopic effect of large-scale moisture transport. The precipitation $\delta^2\text{H}$ accompanying the well-organized convection type decreased significantly by about 20 per mil. Drastic changes in isotope ratios could be described by the Rayleigh distillation process. Isotope ratios of precipitation gently decreased and subsequently increased in the unorganized convection type since the water vapor in surrounding convectively rising air isotopically enriched the remaining low-isotope water vapor advected from the precedent clouds. Isotope ratios in the stratiform precipitation remained steady, possibly attributable to the homogeneous moisture of stratiform clouds.

1. Introduction

Stable hydrogen and oxygen isotope ratios ($\delta^2\text{H}$ and $\delta^{18}\text{O}$) of precipitation undergo temporal changes at various time scales. Many isotopic studies have observed long-term isotopic changes in precipitation in time periods of more than a day or several hours (e.g., Ichiyanagi et al. 2005). Such long-term isotopic changes in precipitation may be controlled by large-scale moisture transport, i.e., the water source and transport route. However, the behavior of precipitation isotope ratios is also intimately linked to precipitation growth mechanisms, namely precipitation/cloud processes (mesoscale processes). Isotopic fractionation in clouds occurs during evaporation and condensation of water vapor and precipitating particles, with the exception of the sublimation and melting of compact ice (e.g., Dansgaard 1953). Mesoscale processes may cause short-term isotopic changes with time scales of less than few hours.

Drastic decreases in precipitation isotope ratios have often been observed during individual precipitation events at various sites (e.g., Sugimoto and Higuchi 1988; Lawrence et al. 1998; Gedzelman et al. 2003). Sugimoto and Higuchi (1988) reported large (small) decreases in precipitation isotope ratios when the precipitation intensity was high (low). Fudeyasu et al. (2008) found increases in the isotope ratios of precipitation accompanying a tropical cyclone eyewall. Dansgaard (1953) ob-

served that isotopic ratios in precipitation did not vary with time throughout a rain shower. More recently, Risi et al. (2009) also reported on an isotopic observational campaign and analyzed the isotope ratios of precipitation accompanying four squall lines over the Sahel in August 2006. Their high-frequency sampling (5–10 minutes) of the precipitation showed a systematic evolution of precipitation isotope ratios in different phases of the squall lines.

The various mesoscale processes, characterized by different precipitation types (convective and stratiform precipitation) and cloud structures, could contribute to the variability in short-term isotopic changes in precipitation. Although previous isotopic observations have provided much information on individual precipitation events, few studies have demonstrated how the isotopic effects of large-scale moisture transport and mesoscale processes simultaneously contribute to the isotope composition in precipitation. This may reflect the lack of long-term precipitation sampling at high temporal resolutions or the difficulty of simultaneously capturing cloud processes, or both. Therefore, we conducted a 1-month intensive isotopic observation of precipitation samples taken at 1-mm amount intervals and 6-hourly intervals on the west coast of Sumatera, Indonesia (Fig. 1), in November 2006 during the intense observation period of the Hydrometeorological ARray for Intraseasonal Variation-Monsoon AUtomonitoring (HARIMAU2006). The compre-

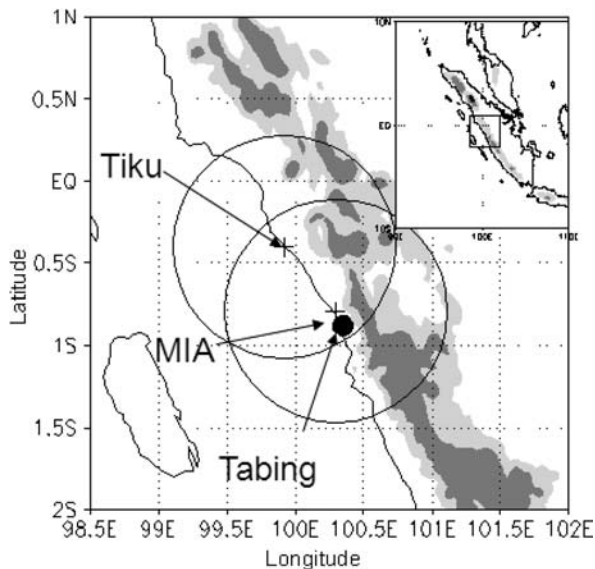


Fig. 1. Terrain map of Sumatera Island and location of observation sites. Altitudes of 500–1,000 m are lightly shaded, while those above 1,000 m are heavily shaded. The dot indicates the isotopic and meteorological observation site at Tabing. Crosses indicate the XDR observation sites at MIA and Tiku. The open circles show the MIA-XDR and Tiku-XDR observation area.

hensive meteorological and radar observations conducted during the HARIMAU2006 were aimed at better understanding cloud structures. The purpose of present study is to investigate how large-scale moisture transport and mesoscale processes influence the variability of precipitation isotope ratios. Notably, this is the first report to describe the high-resolution measurement of isotope ratios in tropical precipitation together with comprehensive meteorological observations and an isotope circulation model that not only captured the large-scale moisture transport but also mesoscale processes over the tropics.

The rest of the paper is organized as follows. The next section briefly describes the isotopic and meteorological observations and the isotope circulation model. Section 3 presents the observed intraseasonal isotopic changes controlled by large-scale moisture transport. Section 4 discusses the variability of precipitation isotope ratios in several precipitation events. The main findings are summarized in the last section.

2. Isotopic and meteorological observations and isotope circulation model

The HARIMAU2006 (Yamanaka et al. 2008), conducted on the west coast of Sumatera (Fig. 1) from 26 October to 27 November 2006, consisted of intensive rawinsonde and surface observations at Tabing (100.4°E, 0.8°S) and dual X-band Doppler radar (XDR) observations at Tiku (Tiku-XDR) and Minangkabau International Airport (MIA-XDR). Surface observations provided 1-minute averages of temperature, relative humidity, winds, pressure, radiation, and accumulated precipitation. Two XDRs collected three-dimensional reflectivity and Doppler velocity data every 6 minutes in observation ranges 83 km in radius. Reflectivity was interpolated on a Cartesian coordinate system with 500-m grid spacing in the horizontal and the vertical. Dual Doppler analysis, using Doppler velocity data and a continuity equation (Ray et al. 1980), provided three components of wind. Additionally, the MIA-XDR results were used in algorithms (Steiner et al. 1995) to objectively classify the precipitation as convective or stratiform (Mori et al. 2011; Kawashima et al. 2011). We also used the equivalent black body temperature (T_{BB}) of satellite images from the geostationary meteorological satellite (MTSAT), to describe the large-scale cloud features. These data were defined on a 0.2° horizontal grid.

Intense isotopic observation was conducted at Tabing from 1 to 27 November 2006. Precipitation samples were automatically collected for every 1-mm amount, with an auto-precipitation sampler to describe short-term isotopic changes. Here, we define “short term” as a period within 6 hours, in which the isotopic variability is affected by mesoscale processes. We stored precipitation samples in sealed bottles promptly after the cessation of a precipitation event to prevent evaporation. In total, 103 complete samples were collected during the HARIMAU2006. We also collected 25 samples at 6-hour intervals to describe intraseasonal isotopic changes. The isotopic composition of samples was analyzed by a MAT-252 analyzer with a water equilibrium device at the laboratory of the Institute of Observational Research for Global Change, Japan Agency for Marine-Earth Science and Technology (JAMSTEC). Analytical errors were less than ± 1 per mil for $\delta^2\text{H}$ and ± 0.1 per mil for $\delta^{18}\text{O}$.

We used isotopic compositions of precipitation simulated by the Rayleigh-type Isotope Circulation

Model (ICM) to detect the effect of large-scale moisture transport (Yoshimura et al. 2003a, b; Yoshimura et al. 2004). The ICM is a type of atmospheric transport model for water isotopes with a horizontal resolution of 1.0° and one vertical layer. The model is driven by global atmospheric analysis fields from the operational weather forecast system of the Japan Meteorological Agency, and the model estimates global distributions of vapor and precipitation isotope ratios at 6-hour intervals. Note that the ICM only focuses on large-scale moisture transport and does not include cloud/precipitation processes.

3. Intraseasonal changes in precipitation isotope ratios

Figure 2a shows the time series of 6-hourly precipitation observed at Tabing from 1 to 27 November 2006. The active period of precipitation started in late November, which is consistent with the previously reported climatological change from the dry to the rainy season (Hamada et al. 2002). Precipitation in late November was also characterized by developed convective precipitation with diurnal variation that peaked in the afternoon, which was consistent with previous studies (Murakami 1983; Nitta and Sekine 1994; Wu et al. 2003; Mori et al. 2004).

Figure 2b shows the time series of precipitation $\delta^2\text{H}$ observed at Tabing. Values of precipitation $\delta^2\text{H}$ ranged from +10 to -65 per mil with an aver-

age of -24 per mil. Using the classifications for convective and stratiform precipitation (Steiner et al. 1995) derived from the analysis of MIA-XDR observations, 42 precipitation samples collected for 1-mm amount were taken during stratiform precipitation, while 61 samples were taken during convective precipitation. The difference in average isotope ratios between stratiform (-22 per mil) and convective (-27 per mil) precipitation was not statistically significant. It means that the isotopic composition of precipitation was independent from difference in precipitation type.

The precipitation $\delta^2\text{H}$ ranged from $+5$ to 0 per mil in early November, whereas low precipitation $\delta^2\text{H}$ of around -40 per mil was observed on 13 November (Fig. 2b). In the following several days, the precipitation $\delta^2\text{H}$ remained relatively low at around -15 per mil. The precipitation $\delta^2\text{H}$ from 21 through 25 November decreased day by day, with a large variability ranging from 0 to -65 per mil. Intraseasonal changes in the precipitation $\delta^2\text{H}$ featured decreases in middle and late November.

Figure 3 shows the time-height section of winds and relative humidity derived from upper air sounding and surface observations at Tabing. At the surface, throughout the entire observation period, south or southwest winds dominated during the day at Tabing. On 13 November, easterlies with high relative humidity of more than 80% started to appear in the mid-troposphere. After several days of inactive precipitation in middle No-

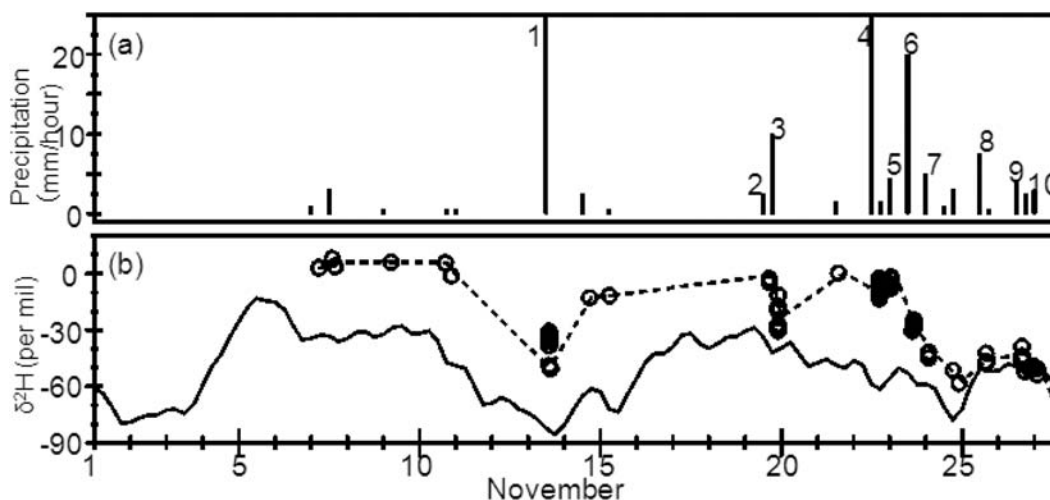


Fig. 2. Time series of observed (a) 6-hourly precipitation and (b) 6-hourly precipitation $\delta^2\text{H}$ (dashed line), 1-mm precipitation $\delta^2\text{H}$ (circle), and simulated 6-hourly precipitation $\delta^2\text{H}$ (solid line). Numerals in (a) indicate the event number shown in Table 1.

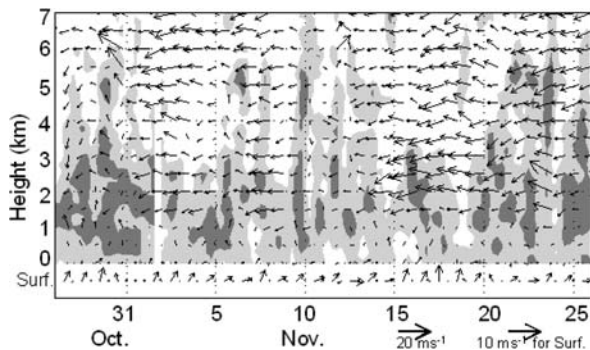


Fig. 3. Time-height section of winds (arrows, scale at bottom) and relative humidity (shaded). Regions with greater than 80 and 90% relative humidity are lightly and heavily shaded, respectively. Surface wind is added at the bottom.

vember, strong easterlies were dominant in the mid-lower troposphere above 2-km height. Figure 4 shows the time-longitude cross-section of MTSAT T_{BB} zonally averaged for $0.5\text{--}1.5^\circ\text{S}$. There were organized cloud clusters at 100°E longitude which corresponded to the precipitation observed at Tabing. In early November, cloud clusters with time scales shorter than a day intermittently appeared around 100°E . In middle and late November, cloud clusters developed around $105\text{--}115^\circ\text{E}$ and moved westward to 100°E with time scales exceeding a few days, typical features in the westward-propagating mesoscale cloud clusters associated with the intraseasonal oscillation (Shibagaki et al. 2006a, b). Therefore, the intraseasonal changes in the precipitation isotope ratios can be considered as a result of the changes in the large-scale environment associated with the intraseasonal oscillation with a time-scale of 10–15 day over Sumatera.

Figure 2b also shows the ICM-simulated precipitation $\delta^2\text{H}$ at the grid point (100.5°E , 0.5°S) near Tabing. Although there is systematic model underestimation in the simulation values due to the lower isotope ratio of evaporation from the sea surface (Yoshimura et al. 2004), the model reproduced the intraseasonal changes with a time-scale of 10–15 day in the observed precipitation $\delta^2\text{H}$ well. The biases between observed and ICM-simulated precipitation $\delta^2\text{H}$ in late November decreased when the amount of observed precipitation increased (Fig. 2a) but the modeled precipitation did not increase so much (not shown). The ICM using under-

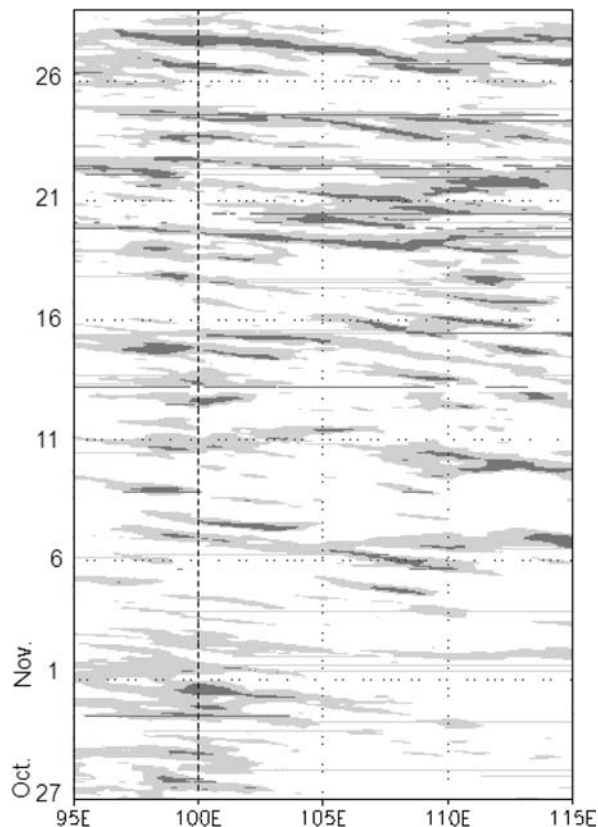


Fig. 4. Time-longitude section of equivalent black body temperature (T_{BB}) zonally averaged in $0.5\text{--}1.5^\circ\text{S}$. Regions with T_{BB} of 220–260 K are lightly shaded, while those with T_{BB} smaller than 220 K are heavily shaded. The broken line indicates the longitude of 100°E .

estimated modeled precipitation simulated gentle decreases in precipitation $\delta^2\text{H}$ in late November due to the lack of amount effect on precipitation isotopes (Lee and Fung 2008). The isotopic changes simulated by the ICM were only affected by large-scale moisture transport, suggesting that the isotopic effect of mesoscale processes on the isotopic averages of each precipitation event was almost masked and only the isotopic effect of large-scale moisture transport became apparent in this time scale.

4. Short-term isotopic variability in precipitation events

Ten precipitation events exceeding 3 mm were observed at Tabing (Table 1 and Fig. 2a). From precipitation types and cloud structures derived

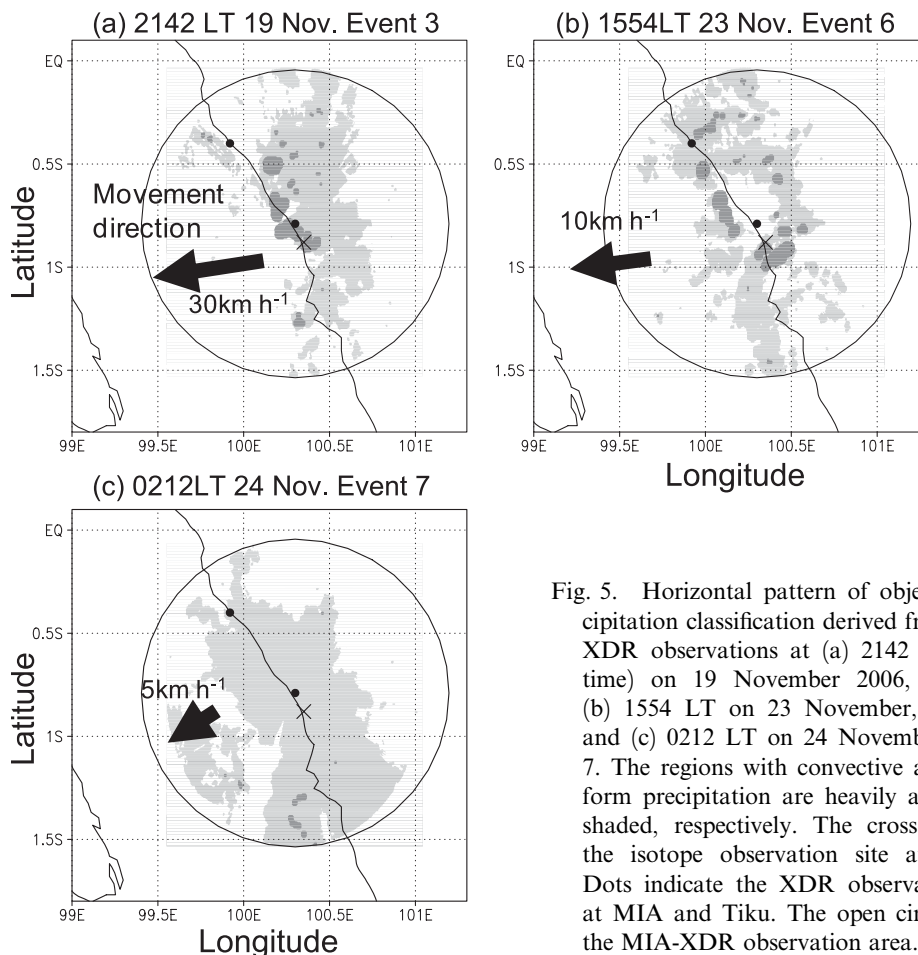


Fig. 5. Horizontal pattern of objective precipitation classification derived from MIA-XDR observations at (a) 2142 LT (local time) on 19 November 2006, Event 3; (b) 1554 LT on 23 November, Event 6; and (c) 0212 LT on 24 November, Event 7. The regions with convective and stratiform precipitation are heavily and lightly shaded, respectively. The cross indicates the isotope observation site at Tabing. Dots indicate the XDR observation sites at MIA and Tiku. The open circle shows the MIA-XDR observation area.

from the analysis of XDR observations, these ten precipitation events were divided into three types: the well-organized convection type, unorganized convection type, and stratiform type. In Event 3, on 19 November, the cloud structure was characterized by an organized convective line developed in the front side of the system with a trailing broad stratiform area (Fig. 5a), referred to as the well-organized convection type. Several convective clouds developed around the region during Event 6 on 23 November (Fig. 5b). These convective clouds were not organized and intermittently passed over Tabing. We refer to this event as the unorganized convection type. In Event 7, on 24 November, widespread stratiform clouds covered the area around Tabing (Fig. 5c), representing the stratiform type.

The average precipitation $\delta^2\text{H}$ values in each precipitation event were related to the intraseasonal isotopic changes as described in Section 3 and

Table 1. It means that the mesoscale isotopic effect of event types on the averaged precipitation $\delta^2\text{H}$ was masked. However, the differences in the precipitation $\delta^2\text{H}$ between the first and last samples in each event were related to event types (Table 1). The difference was larger in the well-organized convection type and smaller in the stratiform type.

Figure 6 shows the time tendency of precipitation $\delta^2\text{H}$ from the first samples in each event. The duration of precipitation in the well-organized convection type had short period about 30 minutes, while those in the stratiform and unorganized convection types were relatively long. The precipitation $\delta^2\text{H}$ in the well-organized convection type decreased significantly by about 20 per mil within first 20 minutes, whereas that in the stratiform type remained steady. The precipitation $\delta^2\text{H}$ in the unorganized convection type decreased at the beginning, followed by increases and finally decreases. The rates were here defined as the changes in precipitation

Table 1. Summary of the features of ten precipitation events. These events were divided into three types of precipitation processes. O: well-organized convection type; U: unorganized convection type; and S: stratiform type. Difference represents the changes in precipitation $\delta^2\text{H}$ between the first and last samples in each event.

Event	Date in Nov.	Event type	Duration (min)	Total number of samples	Average of $\delta^2\text{H}$ (per mil)	Difference (per mil)
1	13	O	40	13	-40.5	-12.3
2	19	S	30	3	-3.9	-0.6
3	19	O	25	8	-21.5	-15.6
4	22	U	73	24	-6.9	-10.3
5	23	U	50	5	-4.9	-5.8
6	23	U	103	14	-28.3	-12.2
7	24	S	81	5	-43.1	-3.2
8	25	U	15	6	-46.5	-5.6
9	26	U	29	5	-45.4	-13.3
10	27	S	85	4	-51.1	-1.7

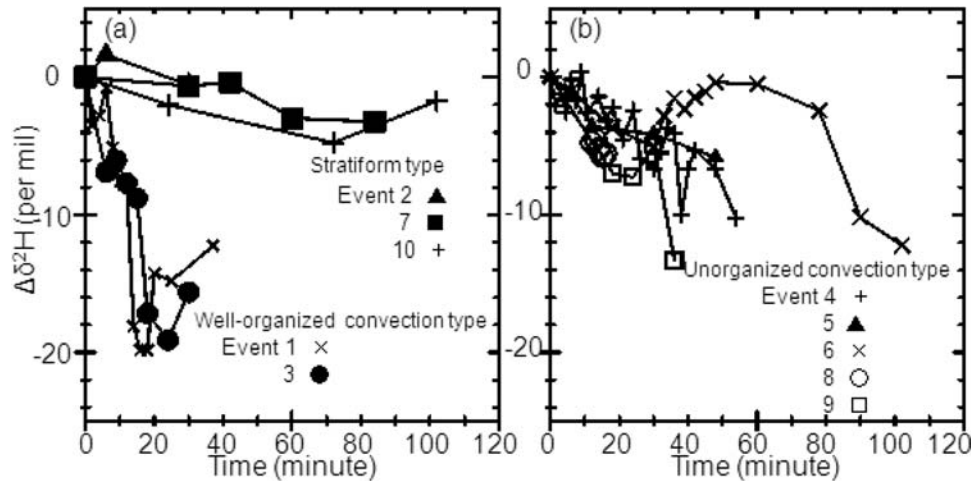


Fig. 6. Time tendency of changes in precipitation $\delta^2\text{H}$ from the first sample for (a) well-organized convection and stratiform types and (b) unorganized convection type.

$\delta^2\text{H}$ divided by the duration of precipitation. The averaged rate in the well-organized convection type was the largest (-0.47 per mil minute^{-1}), whereas that in the stratiform type was the smallest (-0.03 per mil minute^{-1}).

In Event 3, the organized convective clouds quickly moved westward at about 30 km hour^{-1} (Fig. 5a), causing heavy precipitation for 30 minutes and subsequently weak stratiform precipitation at Tabing (Fig. 7). The precipitation $\delta^2\text{H}$ quickly decreased from -11 to -30 per mil. Figure 8 shows a scatter plot of $\delta^{18}\text{O}$ and $\delta^2\text{H}$ values. Samples from Event 3 were plotted above the meteoric water line (MWL; Craig 1961) and decreased over a wide range parallel to the MWL. At the cloud

scale, previous isotopic models using Rayleigh's equation (e.g., Taylor 1972) have attempted to clarify the relationship between $\delta^{18}\text{O}$ and $\delta^2\text{H}$. Taylor (1972) showed that the isotopic composition of subsequent precipitation decreases parallel to the MWL, assuming that the isotopic equilibrium fractionation described by Rayleigh's equation prevails in atmospheric condensation processes, and that the condensed phase is immediately removed from the cloud system without causing isotope exchange between the falling droplets and ambient water vapor, i.e., the kinetic isotopic effect. Therefore, the drastic changes in precipitation isotopic ratios in the well-organized convection type can be interpreted by Rayleigh's distillation process.

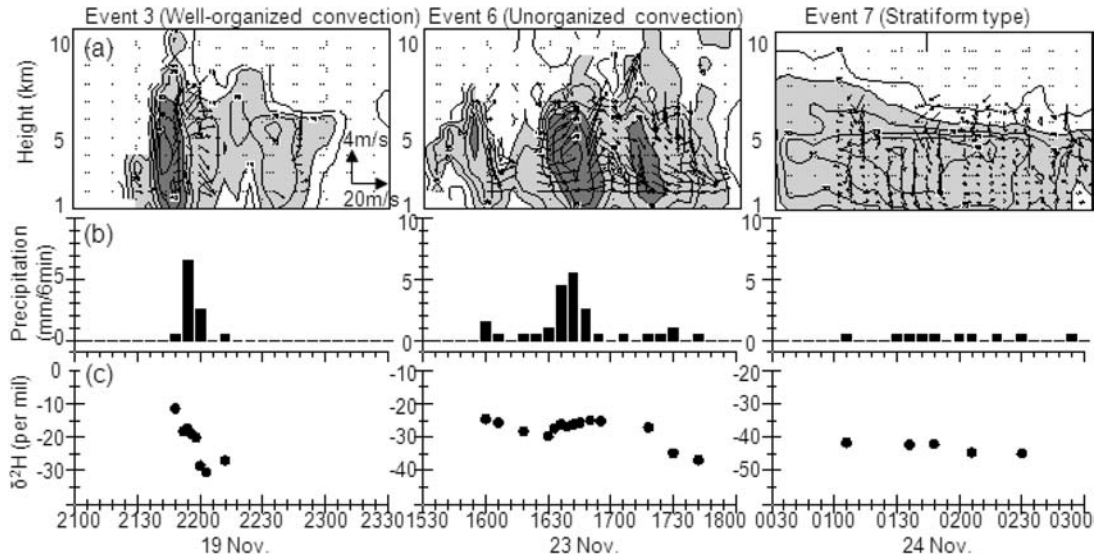


Fig. 7. Time (local time) series of observational results for Events 3, 6, and 7. (a) Reflectivity and system-relative wind (scale at lower right in Event 3), (b) 6-minute precipitation, and (c) precipitation $\delta^2\text{H}$ over Tabing. Regions of 10–20 dBZ reflectivity are lightly shaded, while those more than 20 dBZ are heavily shaded.

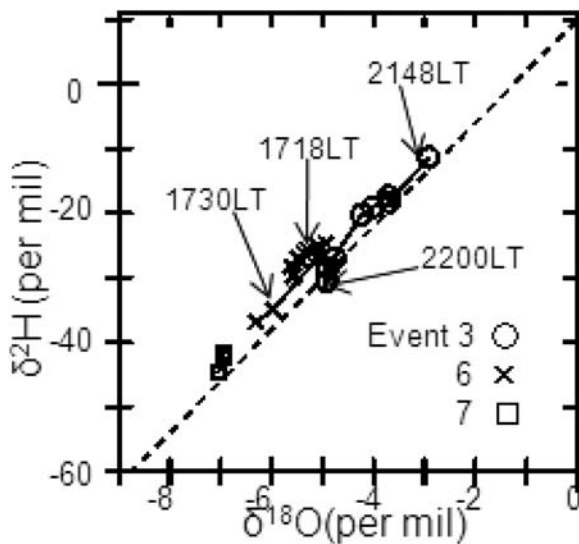


Fig. 8. Scatterplot showing $\delta^{18}\text{O}$ and $\delta^2\text{H}$ for Events 3, 6, and 7. The dashed line denotes the meteoric water line.

Figure 7a shows the reflectivity over Tabing derived from MIA-XDR and system-relative winds derived from dual Doppler analysis. Unfortunately, wind data over Tabing were not complete because of deficiencies in the Doppler velocity observed by Tiku-XDR due to precipitation attenuation. At

2148 local time (LT), system-relative winds in convective cloud showed an upward-motion trend beginning in the lower troposphere and then extending into the trailing stratiform region in the mid-troposphere after 2200 LT. Therefore, the continuous depletion of water vapor isotopes in saturated rising air decreased isotope ratios in the convective precipitation. Stratiform precipitation then formed from the remaining water vapor with lower isotope ratios, leading to the lowest precipitation isotope ratios. The three-dimensional wind field over Tabing derived from dual Doppler analysis revealed the isotopic effect of quasi two-dimensional processes. The quick propagation of the squall line over the observation site also caused quick decreases in the precipitation isotope ratios. The same situation appeared in Event 1 (not shown).

On the other hand, in the unorganized convection type in Event 6, the precipitation $\delta^2\text{H}$ gently decreased and subsequently increased around -25 per mil until 1718 LT (Fig. 7). The unorganized convection type should be three-dimensional system and the water vapor was entrained to the subsequent clouds over Tabing from various directions. Since water vapor from the lower troposphere has relatively high isotope ratios (e.g., Dansgaard 1953), surrounding convectively rising air originating from the lower troposphere isotopically en-

riched the remaining low-isotope water vapor advected from the precedent cloud, slowing the decrease in isotope ratios in subsequent precipitation (Fig. 7c). After convective clouds passed, the precipitation $\delta^2\text{H}$ in the subsequent stratiform precipitation after 1730 LT significantly decreased from -27 to -36 per mil, as described by Rayleigh's distillation process, because of the isotopic changes parallel to the MWL (Fig. 8).

In event 7, the widespread stratiform clouds slowly moved westward (Fig. 5c), causing precipitation for 2 hours at Taping (Fig. 7). The precipitation $\delta^2\text{H}$ also remained steady at around -43 per mil. Dual Doppler observations revealed weak winds in the stratiform clouds and the absence of convective updrafts. Therefore, the steadiness of the isotope ratios in the stratiform precipitation may be attributable to the homogeneous moisture of stratiform clouds.

There were no remarkable changes in deuterium excess (d-excess, $\text{d-excess} = \delta^2\text{H} - 8\delta^{18}\text{O}$) during each precipitation event (not shown). The main physical process causing changes in d-excess is the kinetic isotopic effect, while the production of precipitation from water vapor essentially conserves the d-excess (e.g., Craig 1961). From our observation, the kinetic isotopic effect on the short-term isotopic changes in precipitation was insignificant, compared with the isotopic effects of precipitation/cloud processes. Due to limitations of the observational data, quantitative understanding of these isotopic effects on short-term changes in precipitation isotope ratios remains unclear. Examination of these isotopic effects should be considered for future study.

5. Summary

This study has described the isotopic variability in response to isotopic effects of large-scale moisture transport and mesoscale processes, observed on the west coast of Sumatera, Indonesia, from 1 to 27 November 2006. The precipitation $\delta^2\text{H}$ had large variability, ranging from $+10$ per mil to -65 per mil. Intraseasonal changes in the precipitation $\delta^2\text{H}$ in November were resulted from the changes in the large-scale environment associated with the intraseasonal oscillation with a time-scale of 10–15 day over Sumatera, namely the large-scale moisture transport. Isotopic composition of precipitation was independent from difference in precipitation type. The ICM-simulated precipitation $\delta^2\text{H}$ at the point near Taping reproduced the observed intra-

seasonal isotopic changes, supporting the premise that the isotopic effect of large-scale moisture transport was the main contributory factor of the intraseasonal isotopic changes.

High-frequency sampling of precipitation and radar observations revealed the short-term isotopic variability in precipitation in several precipitation events. Isotopic ratios of precipitation accompanying the well-organized convection type decreased significantly by about 20 per mil, resulting from the continuous depletion of water vapor isotopes in the convectively rising air. Isotope ratios in organized convective precipitation underwent drastic changes which could be described by Rayleigh's distillation process. In the unorganized convection type, the precipitation $\delta^2\text{H}$ gently decreased and then increased since the water vapor in surrounding convectively rising air isotopically enriched the remaining low-isotope water vapor advected from the precedent clouds. Isotope ratios in the stratiform precipitation remained steady, which could be attributable to the homogeneous moisture of stratiform clouds.

The findings suggest that the isotopic effect of mesoscale processes on the isotopic average of each precipitation event was almost masked by the isotopic effect of large-scale moisture transport. However, the short-term isotopic variability, with the exception of intraseasonal isotopic changes, was related to event type classified by the analysis of radar observations. The study results are very encouraging since the short-term isotopic frequency can capture the features of mesoscale processes. Therefore, high-frequency isotopic observation can be applied as a diagnostic tool to understand the precipitation type and cloud structure in individual precipitation events.

Acknowledgments

The authors would like to thank Drs. Naoyuki Kurita and Shingo Shimizu for their helpful comments and supports of data analysis. The authors are also grateful for the assistance of staff members of the Agency for the Assessment and Application of Technology (BPPT) and the Indonesian Meteorological and Geophysical Agency (BMG; now the Indonesian Meteorological Climatological and Geophysical Agency, BMKG) on the Indonesian side and of JAMSTEC, Hokkaido University, and Kyoto University on the Japanese side. This work was supported by the Japan Earth Observation System Promotion Program (JEPP) of the Ministry of

Education, Culture, Sports, Science and Technology, (MEXT), Japan.

References

- Craig, H., 1961: Isotopic variations in meteoric waters. *Science*, **133**, 1702–1703.
- Dansgaard, W., 1953: The abundance of ^{18}O in atmospheric water and water vapor. *Tellus*, **5**, 461–469.
- Fudeyasu, H., K. Ichiyanagi, A. Sugimoto, K. Yoshimura, A. Ueta, M. D. Yamanaka, and K. Ozawa, 2008: Isotope ratios of precipitation and water vapor observed in Typhoon Shanshan. *J. Geophys. Res.*, **113**, D12113, doi:10.1029/2007JD009313.
- Gedzelman, S. D., J. R. Lawrence, J. Gamache, M. Black, E. Hindman, R. Black, J. Dunion, H. Willoughby, and X. Zhang, 2003: Probing hurricanes with stable isotopes of rain and water vapor. *Mon. Wea. Rev.*, **131**, 1111–1127.
- Hamada, J.-I., M. D. Yamanaka, J. Matsumoto, S. Fukao, P. A. Winarso, and T. Sribimawati, 2002: Spatial and temporal variations of the rainy season over Indonesia and their link to ENSO. *J. Meteor. Soc. Japan*, **80**, 285–310.
- Ichiyanagi, K., K. Yoshimura, and M. D. Yamanaka, 2005: Validation of changing water origins over Indochina during the withdrawal of the Asian monsoon using stable isotopes. *SOLA*, **1**, 113–116.
- Kawashima, M., Y. Fujiyoshi, M. Ohi, T. Honda, S. Mori, N. Sakurai, Y. Abe, W. Harjupa, F. Syamsudin, and M. D. Yamanaka, 2011: Case study of an intense wind event associated with a mesoscale convective system in west Sumatera during the HARIMAU2006 campaign. *J. Meteor. Soc. Japan*, **89A**, 239–257.
- Lawrence, J. R., S. D. Gedzelman, X. Zhang, and R. Arnold, 1998: Stable isotopes of rain and vapor in 1995 hurricanes. *J. Geophys. Res.*, **103** (D10), 11,381–11,300.
- Lee, J. E., and I. Fung, 2008, “Amount effect” of water isotopes and quantitative analysis of post-condensation processes, *Hydrol. Process.*, **22**, 1–8.
- Mori, S., J.-I. Hamada, Y. I. Tauhid, M. D. Yamanaka, N. Okamoto, F. Murata, N. Sakurai, H. Hashiguchi, and T. Sribimawati, 2004: Diurnal land–sea rainfall peak migration over Sumatera Island, Indonesian maritime continent, observed by TRMM satellite and intensive rawinsonde soundings. *Mon. Wea. Rev.*, **132**, 2021–2039.
- Mori, S., J.-I. Hamada, N. Sakurai, H. Fudeyasu, M. Kawashima, H. Hashiguchi, F. Syamsudin, A. A. Arbain, R. Sulistyowati, J. Matsumoto, and M. D. Yamanaka, 2011: Convective systems developed along the coastline of Sumatera Island, Indonesia, observed with an X-band Doppler radar during the HARIMAU2006 campaign. *J. Meteor. Soc. Japan*, **89A**, 61–81.
- Murakami, M., 1983: Analysis of deep convective activity over the western Pacific and southeast Asia. Part I: Diurnal variation. *J. Meteor. Soc. Japan*, **61**, 60–76.
- Nitta, T., and S. Sekine, 1994: Diurnal variation of convective activity over the tropical western Pacific. *J. Meteor. Soc. Japan*, **72**, 627–641.
- Ray, P. S., C. L. Ziegler, W. Bumgarner, and R. J. Serafin, 1980: Single- and multiple-Doppler radar observations of tornadic storms. *Mon. Wea. Rev.*, **108**, 1607–1625.
- Risi, C., S. Bony, F. Vimeux, M. Chong, and L. Descroix, 2009: Evolution of the stable water isotopic composition of the rain sampled along Sahelian squall lines. *Quart. J. Roy. Meteor. Soc.*, doi:10.1002/qj.485.
- Shibagaki, Y., T. Shimomai, T. Kozu, S. Mori, Y. Fujiyoshi, H. Hashiguchi, M. K. Yamamoto, S. Fukao, and M. D. Yamanaka, 2006a: Multi-scale convective systems associated with an intraseasonal oscillation over the Indonesian maritime continent. *Mon. Wea. Rev.*, **134**, 1682–1696.
- Shibagaki, Y., T. Kozu, T. Shimomai, S. Mori, F. Murata, Y. Fujiyoshi, H. Hashiguchi, and S. Fukao, 2006b: Evolution of a super cloud cluster and the associated wind fields observed over the Indonesian maritime continent during the first CPEA Campaign. *J. Meteor. Soc. Japan*, **84A**, 19–31.
- Steiner, M., R. A. Houze Jr., and S. E. Yuter, 1995: Climatological characterization of three-dimensional storm structure from operational radar and rain gauge data. *J. Appl. Met.*, **34**, 1978–2007.
- Sugimoto, A., and K. Higuchi, 1988: Relationship between δD and $\delta^{18}\text{O}$ values of falling snow particles from a separate cloud, *Tellus*, **40B**, 205–213.
- Taylor, C. B., 1972: The vertical variations of the isotopic concentrations of tropospheric water vapor over continental Europe and their relationship to tropospheric structure, N. Z. Dep. Sci. Ind. Res., Inst. Nucl. Sci., Rep. INS-R-107: 45pp.
- Wu, P., J.-I. Hamada, S. Mori, Y. I. Tauhid, and M. D. Yamanaka, 2003: Diurnal variation of precipitable water over a mountainous area of Sumatera Island. *J. Appl. Meteor.*, **42**, 1107–1115.
- Yamanaka, M. D., H. Hashiguchi, S. Mori, P. Wu, F. Syamsudin, T. Manik, J.-I. Hamada, M. K. Yamamoto, M. Kawashima, Y. Fujiyoshi, N. Sakurai, M. Ohi, R. Shirooka, M. Katsumata, Y. Shibagaki, T. Shimomai, Erlansyah, W. Setiawan, Bambang Tejasukmana, Yusuf S. Djajadihardja, and J. T. Anggadiredja, 2008: HARIMAU radar-profiler network over the Indonesian maritime continent: A GEOSS early achievement for hydrological cycle and disaster prevention. *J. Dis. Res.*, **3**, 78–88.

- Yoshimura, K., T. Oki, N. Ohte, and S. Kanae, 2003a: A quantitative analysis of short-term ^{18}O variability with a Rayleigh-type isotope circulation model. *J. Geophys. Res.*, **108(D20)**, 4647, doi:10.1029/2003JD003477, 2003.
- Yoshimura, K., T. Oki, N. Ohte, and M. Koike, 2003b: Development and verification of a vertical integrated two dimensional water isotope circulation model. *J. Hydrosci. and Hydraul. Eng.*, **21**, pp. 25–35.
- Yoshimura, K., T. Oki, and K. Ichiyonagi, 2004: Evaluation of two-dimensional atmospheric water circulation fields in reanalyses by using precipitation isotopes databases. *J. Geophys. Res.*, **109(D20)**, doi:10.1029/2004JD004764.